Adaptive HJI Sliding Mode Control of Three Dimensional Overhead Cranes

Zhang Shengzeng, He Xiongxiong

1. Zhejiang University of Technology, Hangzhou 310023
E-mail: 1606226006@qq.com

Abstract: This paper develops an adaptive version of HJI sliding mode controller for the overhead cranes. It deals with the effects of actuator saturation and the presence of disturbances based on RBF neural networks. The sufficient condition under which the overhead crane system is robustly dissipative is proposed using Hamilton-Jacobi-Issacs inequality(HJI) approach. The controller can simultaneously move the trolley and the bridge to their destinations, reduce cargo vibrations during transfer and eliminate cargo swings at the trolley and bridge destinations. The simulation results indicate that the proposed controller asymptotically stabilize all system responses.

Key Words: overhead crane, HJI, neural networks, input saturation

1 INTRODUCTION

For increasing the productivity, the overhead cranes nowadays are usually operated at high speed and it leads to elicited considerable attention on crane control studies. Suspended cargos in overhead crane system are caused to swing without good control strategies and due to the disturbances by open conditions, which can make inaccurate motions of crane mechanisms and the unsafe situation in operation zones. Therefore, it is crucial for overhead crane systems to satisfy rigorous requirements in terms of safety and efficiency.

Up to now, the synthesis of feedback control for overhead cranes remains a challenge since the overhead crane system is under-actuated where the control inputs are lower than that of the number of degrees of freedom. Sliding mode control for a class of under-actuated systems offers a good capability to achieve high tracking performance and preserve strong robustness. The methodology is to keep exactly a properly chosen dynamic constraint in conjunction with high-frequency control switching. Le[1] proposed an adaptive control law for three-dimensional overhead cranes without priori information of cargo mass and friction factors. Liu[2] developed the sliding mode control based on linearized mathematical model by combination of fuzzy logic. Unfortunately, high-frequency control switching in standard sliding mode causes the undesired chattering effect and it keeps the sliding function equal to zero only if the relative degree of the outputs is one. A higher-order sliding mode controller applied for overhead cranes was designed by Raja[3] which can remove the relative degree restriction and has the capability of actuator chattering alleviation. Well, it is assumed that the second-order derivative of the sliding function and the derivative of control signal are bound and it is a tough work to find out the upper limit. There also have been many domestic articles related to the control of overhead cranes. Wang[4] discussed a fuzzy logic-based and anti-sway and positon control for payload-cart system. Yang[5] recommended a radial basis function neural network control of overhead cranes considering the nonlinearity and uncertainty of the model. But it takes more time to execute the duties because of over reliance on samples. Sun[6] provided an adaptive trajectory tracking controller for 3-dimensional overhead cranes. The controller is put forward without approximately decoupling or linearizing the complicated nonlinear model, while the cable length of the model is constant. Zhang[7] calculated a symmetric 3-humps extra insensitive input shaper developed for the variable pendulum length case by vector calculation and it is also shown that input shaping has the suppression function for payload swings.

Due to the restrictions of the actuator, the control inputs are usually bounded by a known constant, and it is difficult to achieve large control signals. Besides, the presences of uncertainties and disturbances may cause poor qualities of the controller in operating environment. In case of this, an adaptation mechanism based on RBF neural networks is constructed to adjust the unknown factors. The system stability is investigated using HJI theory. The qualities of the control algorithm are verified by numerical simulation.

2 MODELLING OF OVERHEAD CRANES

The overhead crane system considered in this study consists of four masses as visualized in Figure 1, namely cargo, trolley, bridge and equivalent of all rotating components of hoist. The bridge is a distributed beam whose mass is converted into a lumped mass m_b set in the bridge center, the equivalent mass of hoist mechanism is represented by m_l, m_t and m_c are masses of trolley and cargo, respectively. The crane system motion is represented by five generalized coordinates: in which, $x(t)$ is trolley displacement, $y(t)$ indicates bridge movement along Oy axis,

This work is supported by National Nature Science Foundation under Grant No. 60875055.

l is the length of the rope, φ is the tangential pendulaion and θ is the radial sway caused by the motion of the cargo. Hence, the positions are described by $q = [x\ y\ l\ \varphi\ \theta]$, The control signals u_b u_t and u_l respectively indicate bridge-moving force, trolley-traveling force and cargo lifting motions force. The frictions of wire ropes, trolley and bridge motions are ignored in this paper.

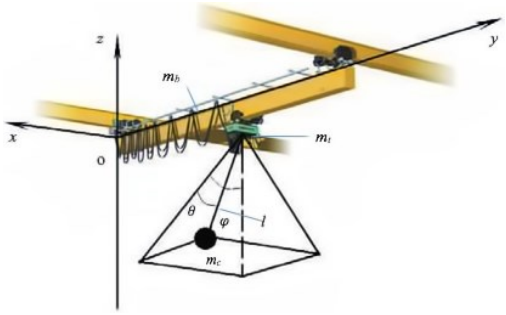

Fig. 1: The overhead crane system

Based on the virtual power principle and Lagrange theory, the equation describing the crane dynamics can be casted in the form of

$$\mathrm{M(q)}\ddot{q} + C(q,\dot{q}) + G(q) + D = U \tag{1}$$

Where, $M(q) = M^T(q)$ is symmetric mass matrix. $C(q,\dot{q})$ is the Centrifugal-Coriolis, G(q) is the gravity vector. F is called vector of control forces of actuators. The system matrices are obtained by the following formulas:

$$M(q) = \begin{bmatrix} m_{11} & 0 & m_{13} & m_{14} & m_{15} \\ 0 & m_{22} & m_{23} & 0 & m_{25} \\ m_{31} & m_{32} & m_{33} & 0 & 0 \\ m_{41} & 0 & 0 & m_{44} & 0 \\ m_{51} & m_{52} & 0 & 0 & m_{55} \end{bmatrix},$$

$$C(q,\dot{q}) = \begin{bmatrix} 0 & 0 & c_{13} & c_{14} & c_{15} \\ 0 & 0 & c_{23} & 0 & c_{24} \\ 0 & 0 & 0 & c_{34} & c_{35} \\ 0 & 0 & c_{43} & c_{44} & c_{45} \\ 0 & 0 & c_{53} & c_{54} & c_{55} \end{bmatrix},$$

$G(q) = [0, 0, g_3, g_3, g_5]^T$,

$\mathrm{D}(q) = [\mathrm{d}_1, \mathrm{d}_2, \mathrm{d}_3, 0, 0]^T$, $U = [u_b, u_t, u_l, 0, 0]^T$.

The coefficients of M(q) matrix are determined as follows.

$m_{11} = m_t + m_b + m_c$, $m_{13} = m_{31} = m_c sin\varphi sin\theta$,

$m_{14} = m_{41} = m_c lcos\varphi cos\theta$, $m_{22} = m_t + m_c$,

$m_{15} = m_{51} = -m_c lcos\varphi cos\theta$, $m_{33} = m_c + m_l$,

$m_{44} = m_c l^2 cos\theta$, $m_{25} = m_{52} = m_c lcos\theta$.

$m_{55} = m_c l^2$.

The coefficients of $C(q,\dot{q})$ matrix are given by the below equations.

$c_{13} = m_c cos\varphi cos\theta\dot{\varphi} - m_c sin\varphi sin\theta\dot{\theta}$,

$c_{14} = m_c cos\varphi cos\theta\dot{l} - m_c lcos\varphi sin\theta\dot{\theta} - m_c lsin\varphi cos\theta\dot{\varphi}$,

$c_{15} = -m_c lcos\varphi sin\theta\dot{\varphi} - m_c sin\varphi sin\theta\dot{l} - m_c lsin\varphi cos\theta\dot{\theta}$,

$c_{25} = m_c cos\theta\dot{l} - m_c lsin\theta\dot{\theta}$, $c_{34} = -m_c lcos^2\theta\dot{l}$,

$c_{35} = -m_c l\dot{\theta}$, $c_{44} = m_c lcos^2\theta\dot{l} - m_c l^2 cos\theta sin\theta\dot{\theta}$,

$c_{45} = -m_c l^2 cos\theta sin\theta\dot{\varphi}$, $c_{53} = m_c l\theta$,

$c_{54} = m_c l^2 cos\varphi sin\theta\dot{\varphi}$, $c_{55} = m_c l\dot{l}$, $c_{23} = m_c cos\theta\dot{\theta}$.

The nonzero coefficients of G(q) vector are written as

$g_3 = -m_c g cos\varphi cos\theta$, $g_4 = m_c glsin\varphi cos\theta$,

$g_5 = m_c glcos\varphi sin\theta$.

The nonzero coefficients of D vector are obtained as $d_1 = 3signx$, $d_2 = 3signy$. $d_3 = 3signl$.

Where g is the gravitational acceleration. The input vector U and the vector of generalized coordinates q are respectively characterized as $\mathrm{U} = [u_b, u_t, u_l, 0, 0]^T$ and $\mathrm{q} = [x, y, l, \varphi, \theta]^T$. Apparently, the overhead crane system is typically under-actuated with five controlled outputs but only three actuators.

3 ADAPTIVE HJI SLIDING MODE CONTROLLER

The section presents the design of the control algorithm for trajectory tracking and anti-sway control of the overhead crane. The adaptive HJI sliding mode controller design is composed of two phases. First, a control law is designed based on a positive definite solution of HJI approach, Second, since the input saturation and preserving the strong robustness are considered, an adaptation mechanism based on RBF neural networks is proposed to adjust the inputs and uncertain disturbances of the crane system taking advantage of updating to the controller for stabilizing the system responses. Note that the proposed controller together with adaptation structure must well implement five duties composed of precisely driving bridge and trolley to come to their destinations, hoisting the cargo to achieve the desired length of cable, keeping the cargo swing angles small during the transport process, and absolutely suppressing the payload swings at steady state.

3.1 Decoupling

The vectors of generalized coordinates can be partitioned as $q^T = [q_a^T, q_u^T]$ comprising the actuated state vector $q_a$and unactuated state vector q_u . Similarly, we separate the input vector into $U^T = [u^T, 0_{1\times2}^T]$, The partitioned vectors are defined as follows:

$q_a = [x, y, l]^T$, $q_u = [\varphi, \theta]^T$, $\mathrm{u} = [u_b, u_t, u_l]^T$.

Then (1) is rewritten as

$$\mathrm{M_{11}\ddot{q}_a + M_{12}\ddot{q}_u + C_{11}\dot{q}_a + C_{12}\dot{q}_u + G_1 = U} \tag{2}$$

$$\mathrm{M_{21}\ddot{q}_a + M_{22}\ddot{q}_u + C_{21}\dot{q}_a + C_{22}\dot{q}_u + G_2 + D_2 = 0} \tag{3}$$

Where,

$$M_{11} = \begin{bmatrix} m_{11} & 0 & m_{13} \\ 0 & m_{22} & m_{23} \\ m_{31} & m_{32} & m_{33} \end{bmatrix}, M_{12} = \begin{bmatrix} m_{14} & m_{15} \\ 0 & m_{25} \\ 0 & 0 \end{bmatrix},$$

$$M_{21}=\begin{bmatrix} m_{41} & 0 & 0 \\ m_{51} & m_{52} & 0 \end{bmatrix},\ M_{22}=\begin{bmatrix} m_{44} & 0 \\ 0 & m_{55} \end{bmatrix},$$

$$C_{11}=\begin{bmatrix} 0 & 0 & c_{13} \\ 0 & 0 & c_{23} \\ 0 & 0 & 0 \end{bmatrix},\ C_{12}=\begin{bmatrix} c_{14} & c_{15} \\ 0 & c_{25} \\ c_{34} & c_{35} \end{bmatrix},$$

$$C_{21}=\begin{bmatrix} 0 & 0 & c_{43} \\ 0 & 0 & c_{53} \end{bmatrix},\ C_{22}=\begin{bmatrix} c_{44} & c_{45} \\ c_{54} & c_{55} \end{bmatrix}.$$

$$G_1=\begin{bmatrix} 0 \\ 0 \\ g_1 \end{bmatrix},\ G_2=\begin{bmatrix} g_4 \\ g_5 \end{bmatrix},\ D_1=\begin{bmatrix} d_1 \\ d_2 \\ d_3 \end{bmatrix},\ \mathrm{U}=\begin{bmatrix} u_b \\ u_t \\ u_l \end{bmatrix}.$$

The under-actuated states q_u can be obtained from (3) as

$$\ddot{\mathrm{q}}_u=-M_{22}^{-1}(q)(M_{21}(q)\ddot{q}+C_{21}(q,\dot{q})\dot{q}_a+C_{22}(q,\dot{q})\dot{q}_u+G_2(q)) \quad (4)$$

By substituting (4) into (2), we get the following form:

$$\bar{M}\ddot{q}_a+\bar{C}(q,\dot{q})\dot{q}_u+\bar{G}(q)+\bar{D}(q)=\mathrm{U} \quad (5)$$

In which,

$$\bar{M}(q)=M_{11}(q)-M_{12}(q)M_{22}^{-1}(q)M_{21}(q)$$

$$\bar{C}(\mathrm{q},\dot{\mathrm{q}})=C_{12}(q,\dot{q})-M_{12}(q)M_{22}^{-1}(q)C_{22}(q,\dot{q})$$

$$\bar{G}(\mathrm{q})=G_1(q)-M_{12}(q)M_{22}^{-1}(q)G_2(q)$$

$$\bar{D}(\mathrm{q})=D_1$$

After complex calculation, the above mentioned matrices are described as follows

$$\bar{M}(q)=\begin{bmatrix} m_b+m_t+m_c sin^2\varphi sin^2\theta & \frac{1}{2}m_c sin\varphi sin2\theta & m_c sin\varphi sin\theta \\ \frac{1}{2}m_c sin\varphi sin2\theta & m_t+m_c sin^2\theta & m_c sin\theta \\ m_c sin\varphi sin\theta & m_c sin\theta & m_t+m_c \end{bmatrix}$$

$$\bar{C}(q,\dot{q})=-m_c l\begin{bmatrix} sin\varphi cos^3\theta\dot{\varphi} & sin\varphi cos\theta\dot{\theta} \\ cos^2\theta sin\theta\dot{\varphi} & sin\theta\dot{\theta} \\ cos^2\theta\dot{\varphi} & \dot{\theta} \end{bmatrix},$$

$$\bar{G}(q)=-m_c g cos\varphi cos\theta\begin{bmatrix} sin\varphi cos\theta\dot{\theta} \\ sin\theta \\ 1 \end{bmatrix},\ \bar{D}=3\begin{bmatrix} sgn(x) \\ sgn(y) \\ sgn(l) \end{bmatrix}.$$

Mathematical model governed by (4) and (5) will be applied for designing the adaptive HJI sliding scheme in the next section.

3.2 HJI Control Scheme

The tracking and anti-sway problem is constituted in finding a control algorithms guaranteeing that $lim_{t\to\infty}q_a(t)=q_a^d(t)$ and $lim_{t\to\infty}q_u(t)=0$, where $q_a^d(t)$ represents the reference trajectory for the vector of the actuated generalized coordinates. It is assumed here that all the state variables are measurable. The HJI sliding mode algorithm design involves two steps. First, the vector of sliding functions in terms of tracking errors of both actuated states and un-actuated one is defined. Second, the control scheme is designed based on HJI approach so that all states trajectories are pushed to sliding surface and attracted to the reference values on this surface.

Consider the tracking errors

$$e_a=q_a-q_{ad}=[x-x_d,y-y_d,l-l_d]^T$$

and

$$e_u=q_u-q_{ud}=[\varphi,\theta]^T$$

The sliding surface is defined by linearly combining between position and velocity errors,

$$\mathrm{s}=\dot{\mathrm{e}}_\mathrm{a}+\lambda\mathrm{e}_\mathrm{a}+\alpha\mathrm{e}_\mathrm{u} \quad (6)$$

in which, designed parameters λ and α are determined by

$$\lambda=\begin{bmatrix} \lambda_1 & 0 & 0 \\ 0 & \lambda_2 & 0 \\ 0 & 0 & \lambda_3 \end{bmatrix},\ \alpha=\begin{bmatrix} \alpha_1 & 0 \\ 0 & \alpha_2 \\ 0 & 0 \end{bmatrix}.$$

Let us define the feedforward control law as follows

$$\mathrm{U}=\mathrm{u}+\bar{\mathrm{M}}(q)\ddot{q}_{ad}+\bar{C}(q,\dot{q})\dot{q}_{ud}+\bar{G}(q) \quad (7)$$

In which, u is the feedback control input.

Substituting (7) into (5) and simplifying lead to

$$\bar{\mathrm{M}}(q)\ddot{e}_a+\bar{C}(q,\dot{q})\dot{e}_u+\bar{D}(q)=\mathrm{u} \quad (8)$$

Notice that condition (6) and (8) can be equivalently expressed as

$$\begin{cases} \dot{e}_a=s-\lambda e_a-\alpha e_u \\ \bar{M}\dot{s}=\omega+u-\bar{D}(q) \end{cases} \quad (9)$$

Where,

$$\omega=\bar{\mathrm{M}}(\mathrm{q})(\lambda\dot{\mathrm{e}}_\mathrm{a}+\alpha\dot{\mathrm{e}}_\mathrm{u})+\bar{C}(q,\dot{q})\dot{q}_u$$

Furthermore, it is seen that (9) equivalent to

$$\begin{cases} \dot{x}=f(x)+g(x)d \\ z=h(x) \end{cases} \quad (10)$$

Where,

$$\mathrm{f(x)}=\begin{bmatrix} \dot{\mathrm{e}}_\mathrm{a} \\ \frac{1}{\bar{\mathrm{M}}}(\omega-\bar{\mathrm{D}}+\mathrm{u}) \end{bmatrix},\ \mathrm{g(x)}=\begin{bmatrix} 0 \\ -\frac{1}{\bar{\mathrm{M}}} \end{bmatrix},\ d=\bar{D},$$

The space of square-integrable functions is denoted by $\mathcal{L}_2-$ gain J for the purpose of evaluating robustness of the system.

$$\mathrm{J}=\sup_{\|\mathrm{d}\|\neq 0}\frac{\|z\|_2}{\|\mathrm{d}\|_2} \quad (11)$$

Where $\|z\|_2$ is the square norm of a vector $\mathrm{z}\in\mathbb{R}^k$.The smaller the J, the better the controller.

Consider the system (10) and let $\gamma>0$, we have the below implication. There exists a positive definite solution $L(x)\geq 0$ under differentiability conditions, system (10) is said to have L2–gain less than or equal to γ if

$$\dot{\mathrm{L}}\leq\frac{1}{2}\gamma^2\|\mathrm{d}\|^2-\|\mathrm{z}\|^2$$

The feedback control of the system can be obtained once the HJI has been established.

$$\mathrm{u}=-\omega-\frac{1}{\gamma^2}\mathrm{s}-\mathrm{s} \quad (12)$$

3.3 Adaptation Mechanism

In case of the presence of disturbances and control constraints, the neural network tuned online is used to compensate the inputs and the uncertain terms.

Consider the input errors

$$\delta_1=\mathrm{u}-\upsilon$$

It is assumed to exist such that $\mathrm{u}=\mathrm{sat}(\upsilon)$ and the saturation operator $\mathrm{sat}(\cdot)$ is defined as

$$\text{sat(v)} = \begin{cases} u_{max}, & v > u_{max} \\ v, & |v| \le u_{max} \\ -u_{max}, & v < -u_{max} \end{cases}$$

The RBF neural networks are chosen to perform the approximated action. This leads to the representation of the system block diagram as follows :

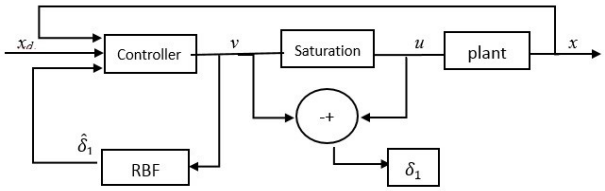

Fig. 2: Overall system block diagram

The RBF neural networks are consisted of inputs and outputs neuron with two hidden layers. The neural network output $\hat{\delta}_1$ is a vector that are obtained on account of the input vector υ. By collecting all the neural network weight into matrices denoted by W, the outputs of neural network can be denoted as

$$\hat{\delta}_1 = \widehat{W}_1{}^T h_1$$

Where the vector h_1 is the outputs of Gauss basis function and the matrices $\widehat{W}_1$ is the estimated weights.

Consider the approaching error

$$\delta_1 - \hat{\delta}_1 = \mathrm{W}_1{}^T \mathrm{h}_1 + \varepsilon_1 - \widehat{\mathrm{W}}_1{}^T \mathrm{h}_1 = -\widetilde{\mathrm{W}}_1{}^T \mathrm{h}_1 + \varepsilon_1$$

Furthermore, it can compensate the factors varied in connection with the open condition based on the neural networks.

$$\delta_2 - \hat{\delta}_2 = \mathrm{W}_2{}^T \mathrm{h}_2 + \varepsilon_2 - \widehat{\mathrm{W}}_2{}^T \mathrm{h}_2 = -\widetilde{\mathrm{W}}_2{}^T \mathrm{h}_2 + \varepsilon_2$$

In case of adaptive control, the control scheme (12) is modified with respect to estimation parameters. The adaptive control inputs derived from (12) are determined by

$$\mathrm{u} = -\omega - \tfrac{1}{\gamma^2}\mathrm{s} - \mathrm{s} + \hat{\delta}_1 + \hat{\delta}_2 \qquad (13)$$

3.4 Stability of the Equivalent System

To demonstrate the stability of the equivalent system by means of control law (13), the following Lyapunov function candidate are chosen.

$$L = \tfrac{1}{2} s^T \bar{M} s + \tfrac{1}{2\eta} tr\left(\widetilde{W}_1{}^T \widetilde{W}_1\right) + \tfrac{1}{2\eta} tr\left(\widetilde{W}_2{}^T \widetilde{W}_2\right) \qquad (14)$$

Then, the derivative of L with respect to time is

$$\begin{aligned} \dot{L} = s^T \bar{M}\dot{s} + \frac{1}{2} s^T \dot{\bar{M}} s + \frac{1}{\eta} tr\left(\dot{\widetilde{W}}_1 \widetilde{W}_1\right) + \frac{1}{\eta} tr\left(\dot{\widetilde{W}}_2 \widetilde{W}_2\right) \\ = s^T(\omega + u - W_1 h_1 - \varepsilon_1 - W_2 h_2 - \varepsilon_2) \\ + \frac{1}{\eta} tr\left(\dot{\widetilde{W}}_1 \widetilde{W}_1\right) + \frac{1}{\eta} tr\left(\dot{\widetilde{W}}_2 \widetilde{W}_2\right) \\ = s^T\left(-\frac{1}{\gamma^2} s - s + \hat{\delta}_1 + \hat{\delta}_2 - W_1 h_1 \right. \\ \left. - \varepsilon_1 - W_2 h_2 - \varepsilon_2\right) + \frac{1}{\eta} tr\left(\dot{\widetilde{W}}_1 \widetilde{W}_1\right) \\ + \frac{1}{\eta} tr\left(\dot{\widetilde{W}}_2 \widetilde{W}_2\right) \\ = s^T\left(-\frac{1}{\gamma^2} s - s - \widetilde{W}_1 h_1 - \varepsilon_1 - \widetilde{W}_2 h_2 \right. \\ \left. - \varepsilon_2\right) + \frac{1}{\eta} tr\left(\dot{\widetilde{W}}_1 \widetilde{W}_1\right) + \frac{1}{\eta} tr\left(\dot{\widetilde{W}}_2 \widetilde{W}_2\right) \end{aligned}$$

Let us define the function H as

$$\mathrm{H} = \dot{L} - \tfrac{1}{2}\gamma^2 \|\varepsilon_1\|^2 - \tfrac{1}{2}\gamma^2 \|\varepsilon_2\|^2 + \|\mathrm{z}\|^2 \qquad (15)$$

Which leads to

$$\mathrm{H} = -s^T\varepsilon_1 - -s^T\varepsilon_2 - \tfrac{1}{\gamma^2} s^T s - s^T s + s^T \widetilde{W}_1 h_1 + s^T \widetilde{W}_2 h_2 + \tfrac{1}{\eta} tr\left(\widetilde{W}_1{}^T \widetilde{W}_1\right) + \tfrac{1}{\eta} tr\left(\widetilde{W}_2{}^T \widetilde{W}_2\right) - \tfrac{1}{2}\gamma^2 \|\varepsilon_1\|^2 - \tfrac{1}{2}\gamma^2 \|\varepsilon_2\|^2 + \|z\|^2$$

Note that

$$-s^T\varepsilon_1 - \frac{1}{2\gamma^2} s^T s - \frac{1}{2}\gamma^2 \|\varepsilon_1\|^2 = -\frac{1}{2}\left\|\frac{1}{\gamma} s + \gamma\varepsilon_1\right\|^2 \le 0$$

$$-s^T\varepsilon_2 - \frac{1}{2\gamma^2} s^T s - \frac{1}{2}\gamma^2 \|\varepsilon_2\|^2 = -\frac{1}{2}\left\|\frac{1}{\gamma} s + \gamma\varepsilon_2\right\|^2 \le 0$$

$$s^T \widetilde{W}_1 h_1 + \frac{1}{\eta} tr\left(\dot{\widetilde{W}}_1{}^T \widetilde{W}_1\right) = 0$$

$$s^T \widetilde{W}_2 h_2 + \frac{1}{\eta} tr\left(\dot{\widetilde{W}}_2{}^T \widetilde{W}_2\right) = 0$$

$$-s^T s + \|\mathrm{z}\|^2 = 0$$

By substituting functions mentioned above to the last equation, it can be shown that

$$\mathrm{H} \le 0$$

or in a more convenient form

$$\dot{\mathrm{L}} \le \frac{1}{2}\gamma^2 \|\varepsilon_1\|^2 + \frac{1}{2}\gamma^2 \|\varepsilon_2\|^2 - \|\mathrm{z}\|^2$$

Applying HJI, one can easily indicates that $\mathrm{J} \le \gamma$ which implies that the surface $\mathrm{s} \to 0$ is globally reached in a finite time.

4 SIMULATION AND RESULTS

The system dynamics shown in (2) and (3) driven by adaptive robust actuators is numerically simulated via MATLAB\SIMULINK programming. In this study the plant parameters are listed as m_c = 0.8 *kg*, m_t = 3 *kg*, m_b = 5 *kg, m_l = 2 kg.* The control law parameters used in the simulations are λ_1 = 0.9, λ_2 = 1.0, λ_3 = 1.1, α_1 = –2, α_2 = –4, The initial values of the generalized coordinates vector are chosen such that $(x, y, l, \varphi, \theta) = (0m, 0m, 1m, 0deg, 0deg)$ and $\mathrm{g} = 9.8065\mathrm{m}/s^2$. The control forces drive bridge to move to 1.0 m displacement, trolley to reach to 1.0 m reference and suspended cargo to be lifted to 3 m desired length. Assume

that the damped aspects are selected to be zeros and the control is set to be bounded by 15, The values of the RBF neural networks parameters are determined by the actual input numbers.

The results are shown in Figs. 3 to 6. These responses illustrated in Fig. 3 asymptotically converge to desired destinations. Trolley motion precisely reach to 1.0 m of endpoint after 10 s. Bridge is tracked to achieve 0.5 m within 10 s. whereas the cable length reaches 1.5 m reference after 5 s. It takes more time to converge the responses to a steady state on account of the bounded of the inputs.

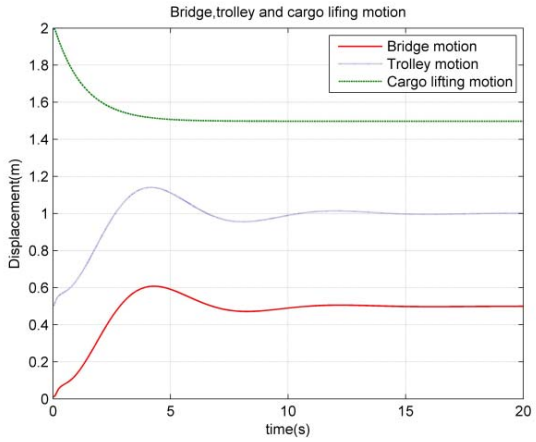

Fig. 3. Displacements of x, y and cable length

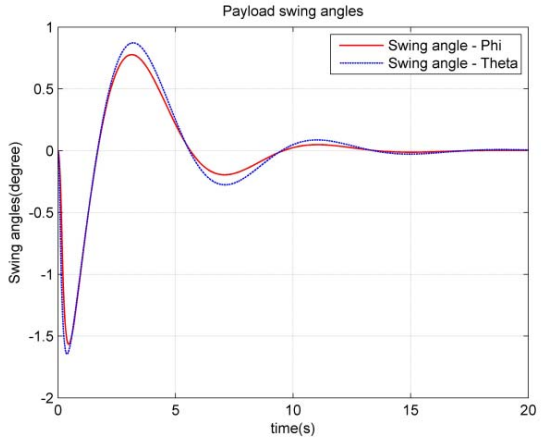

Fig. 4. Cargo swings φ and θ

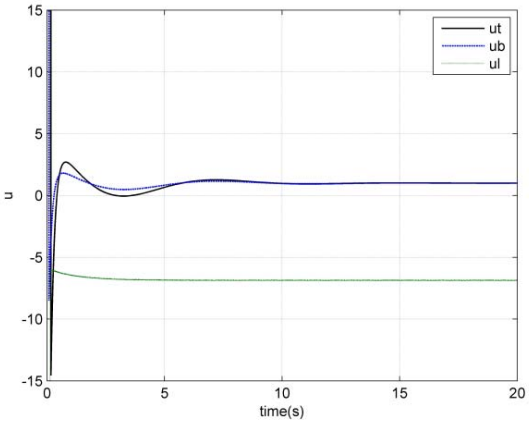

Fig. 5. Control force of bridge, trolley and cable

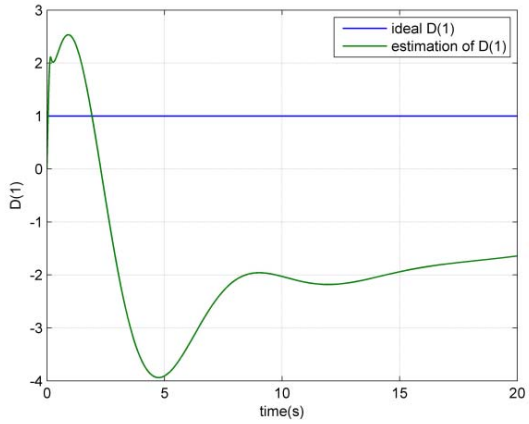

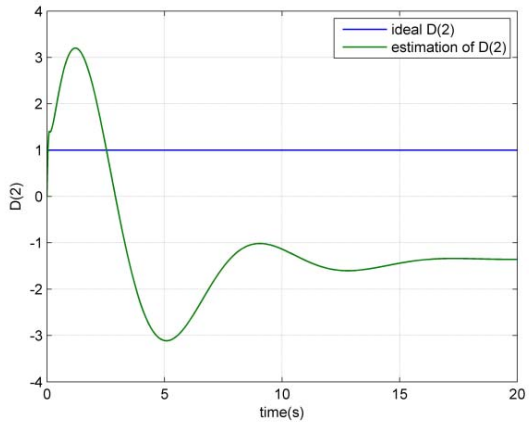

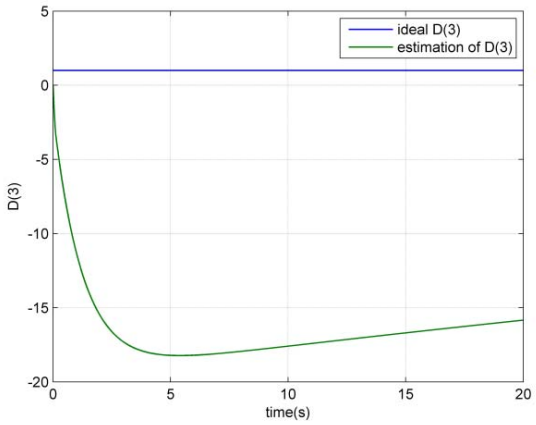

Fig. 6. Estimation of parameters, $\overline{D}$

As shown in Fig. 4, the cargo vibrations depicted in this section are the tangential pendulation and radial sway which are suppressed to the maximum amplitude of 2 degrees and absolutely eliminated at steady states.

Fig. 5 shows that the control inputs are precisely bounded by 15.

Fig. 6 shows the estimation of external disturbances. The estimated parameters are different form the true parameters. This can be explained that the controller is to stabilize asymptotically the system outputs by many values of estimated parameters other than true parameters. The control action does not reflect the important meaning of crane control problem. The main objective of the controller is making the system outputs converged to the stability. Therefore, the convergence of the estimated plant parameters does not bother to discover the true parameters.

5 CONCLUSION

In this paper, an adaptive HJI sliding mode controller is developed for the model of 3D overhead cranes in case of actuator constraint and the presences of disturbances. The asymptotic stability of the closed loop system has been presented based on HJI theory. Robust control performances are obtained when the system is subject to disturbances. The simulation results indicate the effectiveness of the proposed control method. Integrating back-propagation algorithm and observers to adaptive controllers will be developed in future.

REFERENCES

[1] Le Anh Tuan, Sang-Chan Moon, Dong-Han Kim and et al. Adaptive Sliding Mode Control of Three Dimensional Overhead Cranes, IEEE Trans. on CYBER, 354 – 359, 2012.

[2] D. Liu, J. Yi, D. Zhao and W. Wang, Adaptive sliding mode fuzzy control for a two dimensional overhead crane, vol. 15, 505 – 522, 2004.

[3] R. M. T. Raja Ismail, Q. P. Ha, Trajectory Tracking and Anti-Sway Control of Three-dimensional Offshore Boom Cranes Using second-order Sliding Modes, IEEE International Conference on Automation Science and Engineering, 996 – 1001, 2013.

[4] X. J. Wang, H. H. He, Fuzzy Logic –based Anti-Swing and Positon Control for Bridge Cranes, JOURNAL OF SYSTEM SIMULATION, Vol. 17, No. 4, 936 – 939, 2005.

[5] C. Y. Yang, Anti-Swing and Position Control for Bridge Cranes Based on RBF Neural Network, SCIENCEPAPER ONLINE, vol. 6, No. 4, 320 – 324, 2011.

[6] N. Sun, Y. C. Fang, P. C. Wang and X. B. Zhang, Adaptive Tracking Control of Underactuated 3-dimensional Overhead Crane Systems, ACTA AUTOMATICA SINICA, Vol. 36, No. 9, 1287 – 1294, 2010.

[7] X. H. Zhang, Z. Y. Jia, Anti-Swing Control of Ship-mounted Rotary Crane Based on Input Shaping. CONTROL ENGINEERING OF CHINA, Vol. 15, No. 3, 245-249, 2008.

[8] A. J. van der Schaft, L_2-Gain Analysis of Nonlinear Systems and Nonlinear State Feedback H_∞ Control, IEEE Trans. on Automatic Control, Vol, 37, No, 6, 770 – 784, 1992.

[9] J. K. Liu, RBF Neural Network Control for Mechanical Systems Design, Analysis and Matlab Simulation, Tsinghua University Press, Beijing, China, 2014.

[10] J. K. Liu, Sliding Mode Control Design and Matlab Simulation, Tsinghua University Press, Beijing, China, 2012.

[11] Y. C. Chen, Basis of Dynamics of Rigid Bodies, Harbin Ship Engineering Institute Press, Harbin, China, 1995.